The AAPS Journal (2021) 23: 23
DOI: 10.1208/s12248-020-00533-1

Research Article

Population Pharmacokinetics of Intracellular 5-Fluorouridine 5′-Triphosphate and its Relationship with Hand-and-Foot Syndrome in Patients Treated with Capecitabine

Julie M. Janssen,[1,6] Bart A. W. Jacobs,[1] Jeroen Roosendaal,[1] Ellen J. B. Derissen,[1,2] Serena Marchetti,[3] Jos H. Beijnen,[1,4] Alwin D. R. Huitema,[1,5] and Thomas P. C. Dorlo[1]

Received 27 July 2020; accepted 4 November 2020; published online 8 January 2021

Abstract. Capecitabine is an oral pro-drug of 5-fluorouracil. Patients with solid tumours who are treated with capecitabine may develop hand-and-foot syndrome (HFS) as side effect. This might be a result of accumulation of intracellular metabolites. We characterised the pharmacokinetics (PK) of 5-fluorouridine 5′-triphosphate (FUTP) in peripheral blood mononuclear cells (PBMCs) and assessed the relationship between exposure to capecitabine or its metabolites and the development of HFS. Plasma and intracellular capecitabine PK data and ordered categorical HFS data was available. A previously developed model describing the PK of capecitabine and metabolites was extended to describe the intracellular FUTP concentrations. Subsequently, a continuous-time Markov model was developed to describe the development of HFS during treatment with capecitabine. The influences of capecitabine and metabolite concentrations on the development of HFS were evaluated. The PK of intracellular FUTP was described by an one-compartment model with first-order elimination ($k_{e,\mathrm{FUTP}}$ was 0.028 h^{-1} (95% confidence interval 0.022–0.039)) where the FUTP influx rate was proportional to the 5-FU plasma concentrations. The predicted individual intracellular FUTP concentration was identified as a significant predictor for the development and severity of HFS. Simulations demonstrated a clear exposure-response relationship. The intracellular FUTP concentrations were successfully described and a significant relationship between these intracellular concentrations and the development and severity of HFS was identified. This model can be used to simulate future dosing regimens and thereby optimise treatment with capecitabine.

KEY WORDS: 5-fluorouridine 5′-triphosphate; capecitabine; hand-and-foot syndrome; Markov modelling; population pharmacokinetics.

INTRODUCTION

Capecitabine is an oral pro-drug of the anti-cancer drug 5-fluorouracil (5-FU) which is currently registered for the treatment of patients with breast, gastric and colorectal cancer. Following oral administration, capecitabine is rapidly and completely absorbed from the gastro-intestinal tract. Capecitabine is enzymatically converted into 5′-deoxy-5-fluorocytidine (dFCR). dFCR is then converted into 5′-deoxy-5-fluorouridine (dFUR) which is further metabolised into the pharmacologically inactive metabolite 5-FU by thymidine phosphorylase (TP) (1). Approximately 3–5% of 5-FU is intracellularly converted to the cytotoxic metabolites 5-fluoro-2′-deoxyuridine 5′-monophosphate (FdUMP), 5-fluoro-2′-deoxyuridine 5′-triphosphate (FdUTP) and 5-fluorouridine 5′-triphosphate (FUTP) (2). However, 80% of 5-FU is catabolised into the inactive metabolite dihydro-5-FU by dihydropyrimidine dehydrogenase (DPD) and subsequently into the final inactive metabolite fluoro-β-alanine

Supplementary Information The online version contains supplementary material available at https://doi.org/10.1208/s12248-020-00533-1.

[1] Department of Pharmacy & Pharmacology, The Netherlands Cancer Institute - Antoni van Leeuwenhoek, Plesmanlaan 121, 1066 CX, Amsterdam, The Netherlands.
[2] Department of Clinical Pharmacology and Pharmacy, VU University Medical Center, Amsterdam UMC, Amsterdam, The Netherlands.
[3] Department of Clinical Pharmacology, The Netherlands Cancer Institute, Amsterdam, The Netherlands.
[4] Department of Pharmaceutical Sciences, Utrecht University, Utrecht, The Netherlands.
[5] Department of Clinical Pharmacy, University Medical Center Utrecht, Utrecht University, Utrecht, The Netherlands.
[6] To whom correspondence should be addressed. (e–mail: ju.janssen@nki.nl)

(FBAL), which is renally excreted. By binding to the nucleotide-binding site of the nucleotide synthetic enzyme thymidylate synthase (TS), FdUMP disrupts DNA synthesis, which results in DNA damage. In addition, FdUTP can be misincorporated into DNA which leads to DNA strand breaks and cell death. By incorporation into RNA, the 5-FU metabolite FUTP interferes with RNA functionalities (3).

The most commonly observed severe adverse event associated with capecitabine treatment is hand-and-foot syndrome (HFS). The development of HFS may require dose modifications (reduction, interruptions) and/or discontinuation of treatment with capecitabine. In most cases, treatment interruptions followed by dose reductions result in recovery of the symptoms (4). Although several mechanisms for the development of HFS in patients treated with capecitabine have been proposed, the pathophysiology is not yet fully elucidated (4,5). Pressure from walking or use of the hands has been related to the release of capecitabine or its metabolites into surrounding tissue as a result of rupture of the tiny capillaries in the dermis. A previous study showed a decrease in the incidence of HFS during treatment with capecitabine in patients treated with celecoxib compared to patients treated with capecitabine alone, which suggests an inflammatory reaction caused by COX-2 expression in the palms and soles of the hand and the feet, respectively (6–8). Another possible mechanism could be an increased local activation and accumulation of 5-FU and metabolites in the keratinocytes in the skin of the palms and soles as a result of higher TP concentrations in this tissue, as shown by Milano and colleagues (4). As HFS typically develops after several weeks on capecitabine treatment, it is hypothesised that a cumulative drug effect is causing this toxicity. Previous population-based analyses have shown that the development of HFS might be associated with cumulative capecitabine dose administration (9–11). Furthermore, it was shown that a higher incidence of HFS was observed for treatment with capecitabine or prolonged 5-FU infusion compared to bolus 5-FU treatment (9). A significant relationship between capecitabine or metabolite concentrations and severity of HFS has however not been shown (9,10). These studies investigated the predictive value of plasma capecitabine and metabolite concentrations, but did not investigate exposure to intracellular active metabolites.

With this analysis, we aimed to describe the population pharmacokinetics (PK) of the intracellular metabolite FUTP by integration into a previously developed population PK model of capecitabine and the metabolites dFCR, dFUR, 5-FU and FBAL (12). The ultimate goal was to identify whether the intracellular metabolite FUTP is predictive for the development and severity of HFS in patients treated with capecitabine.

MATERIALS AND METHODS

Patients, Study Design and Data

Capecitabine, dFCR, dFUR, 5-FU, FBAL and FUTP PK data were available from patients with solid tumours who participated in two clinical phase I dose-escalation studies and one phase 0 clinical study (13–15). In all three studies, the intracellular FUTP concentrations were determined in peripheral blood mononuclear cells (PBMCs). All studies were approved by the Medical Ethics Committee of the Netherlands Cancer Institute and were performed in compliance with the WHO declaration of Helsinki. In study 1 ($n = 24$ patients with FUTP concentrations available), patients received oral capecitabine twice-daily (BID) in a chronomodulated treatment regimen on days 1–21 of a 21-day cycle. Dose-levels ranged from 375 mg/m^2 in the morning and 625 mg/m^2 in the evening to 950 mg/m^2 in the morning and 1600 mg/m^2 in the evening. Plasma samples were collected at pre-dose, 0.5, 1, 1.5, 2, 3, 5, 11 and15 h after the capecitabine morning dose on day 7 and during the following night (day 8), 0.5, 1, 1.5, 2, 3, 5 and 9 h after the evening capecitabine intake. PBMCs were obtained on day 7 at pre-dose, 1.5 and 3 h after the capecitabine morning dose administration (15). In study 2 ($n = 8$ patients with FUTP concentrations available), patients received capecitabine on days 1–14 of a 21-day cycle. Capecitabine doses ranged from 500 to 1000 mg/m^2 BID. Plasma samples were collected at pre-dose, 1, 2, 3, 4, 6 and 8 h after administration on day 1. PBMCs were obtained on days 1 and 14 of the first cycle at pre-dose, 2, 4, 8 and 12 h after administration (13). In study 3 ($n = 13$ patients with FUTP concentrations available), patients received a single dose of 1000 mg oral capecitabine in the morning. PBMC samples were obtained at pre-dose, 1, 2, 3, 4, 6 and 24 h after administration (14).

Capecitabine, dFCR, dFUR, 5-FU and FBAL concentrations were quantified in plasma using a validated liquid chromatography-tandem mass spectrometry (LC-MS/MS) assay as previously described (16). In all three studies, FUTP concentrations were determined in PBMCs. PBMCs were isolated from peripheral heparinised blood using Ficoll-plaque density gradient and counted using previously described methods (17). The concentrations in PBMCs were calculated based on the amount of the analyte and the number of PBMCs in the obtained lysate.

HFS data was available from study 1 and was assessed weekly during the first treatment cycle and at the end (day 21) of each subsequent cycle. The severity of HFS was graded between 0 and 3, according to the Common Terminology Criteria for Adverse Events (CTCAE) version 4.03.

Intracellular Pharmacokinetic Model

Structural Model

Sequential PK modelling was applied using a previously published population PK model describing the capecitabine, dFCR, dFUR, 5-FU and FBAL plasma concentrations (as shown in Fig. 1) (12). The PK parameters from this model were fixed and used to predict individual capecitabine and metabolite concentrations in plasma while retaining the PK data in the database (18). Effect compartment models and indirect response models were explored for the description of the intracellular FUTP concentrations (19). The intermediate metabolites 5-fluorouridine 5′-monophosphate (FUMP) and 5-fluorouridine 5′-diphosphate (FUDP) were not detectable in the PBMC samples. Therefore, the individual predicted 5-FU concentrations in plasma were used as the driving force for the production of intracellular FUTP concentrations. Linear and Michaelis-Menten (with and without sigmoidicity)

relationships were explored to describe the formation of intracellular FUTP from 5-FU.

Stochastic Model

Inter-individual variability (IIV) was evaluated for all parameters using an exponential model (Eq. 1):

$$P_i = \mathrm{P}_{\mathrm{pop}} \cdot \exp(\eta_i) \quad (1)$$

where the typical population parameter estimate and the individual parameter estimate for individual *i* are represented by P_{pop} and P_i, respectively.

The IIV for subject individual *i* is represented by η_i, which was assumed to be normally distributed following $N\ (0, \omega^2)$. Residual unexplained variability in intracellular FUTP concentrations was described by a proportional error (Eq. 2):

$$C_{\mathrm{obs,ij}} = C_{\mathrm{pred,ij}} \cdot \left(1 + \varepsilon_{p,\mathrm{ij}}\right) \quad (2)$$

where $C_{\mathrm{obs,ij}}$ represents the observed concentration for individual *i* and observation *j*, $C_{\mathrm{pred,ij}}$ represents the individual predicted concentration, and $\varepsilon_{p,\mathrm{ij}}$ represents the proportional error distributed following $N\ (0, \sigma^2)$.

HFS Model

To model the ordered categorical HFS data, a continuous-time Markov transition model (CTMM) was applied (20). CTCAE grades 0 and 1 were grouped into a single category as a result of the low frequency of grade 1 observed and the fact that dose adaptation are indicated from grade 2. This resulted in three different HFS grades (0/1, 2, 3). All patients started with HFS grade 0. Consequently, the initial probability for HFS grade 0/1 was set to 1 for all patients. Thereafter, the model was updated after each observation. To simplify the model, only transitions between neighbouring grades were considered in the analysis. Sequential modelling was used to relate the PK to HFS (18). The individual empirical Bayesian parameter estimates of plasma capecitabine, plasma metabolites and intracellular FUTP PK were fixed and used to derive model-based individual plasma and intracellular concentrations. A common drug effect was tested on each increasing transition rate (k_{01}, k_{12}, k_{23}). The drug effect was firstly introduced as a proportional direct effect by relating predicted concentration (C_p) to the transition rates. Secondly, an indirect effect was tested by using cumulative exposure (area under the concentration-time curve (AUC)) instead of C_p as explanatory factors. Lastly, an effect compartment model including a first-order recovery rate (k_{rec}) was considered. Linear (i.e. proportional) and nonlinear (E_{max}) models were explored to describe the relation between plasma capecitabine, plasma 5-FU and intracellular FUTP concentrations and HFS.

To further assess the clinical impact of the established FUTP-HFS relationship, the final model for HFS was used to simulate the HFS grades for patients treated with the dose-levels that were investigated in study 1 (375/625 mg/m^2, 475/800 mg/m^2, 600/1000 mg/m^2, 750/1250 mg/m^2 and 950/1600 mg/m^2) continuously during 42 days. Doses were administered twice-daily at 09:00 h in the morning and 24:00 h in the evening. For each dose-level, individual FUTP

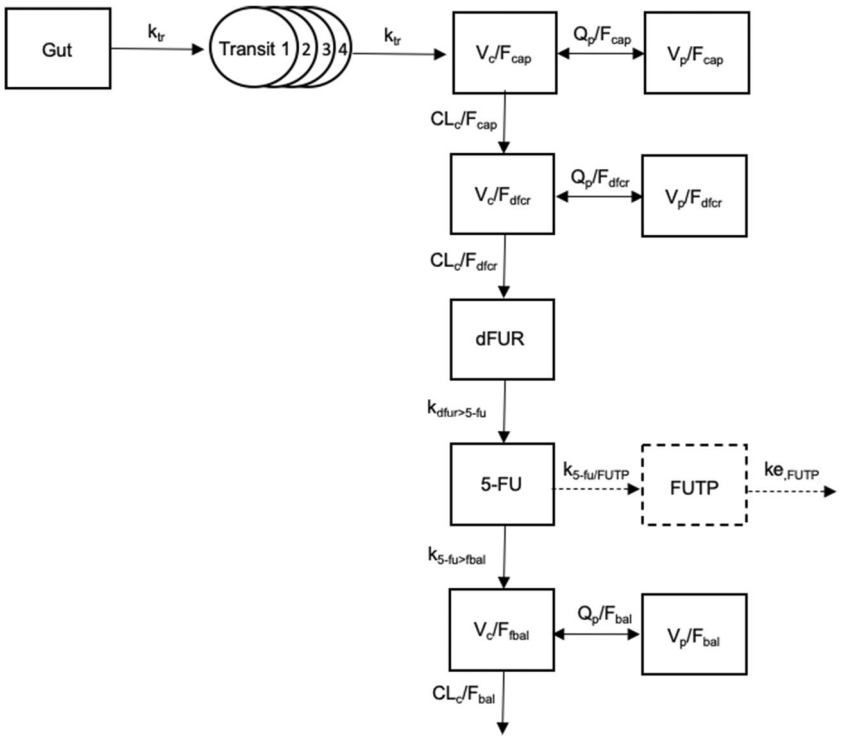

Fig. 1. Schematic representation of the final PK model for plasma capecitabine, dFCR, dFUR, 5-FU and FBAL and intracellular FUTP concentrations

Table I. Population Estimates for the Final Intracellular FUTP Model

	Units	Estimate (95% CI[a])	IIV[b] (95% CI[a]) [Shr%]
Parameter			
$k_{5\text{-FU/FUTP}}$	h^{-1}*fmol/million PBMCs/nM	0.029 (0.028–0.149)	66.0 (53.1–84.8) [2%]
$k_{e,\text{FUTP}}$	h^{-1}	0.028 (0.022–0.039)	–
Residual variability			
Proportional	CV%	38.6 (34.6–44.9)	–

CI, confidence interval; *CV%*, coefficient of variation; *IIV*, inter-individual variability; *Shr*, shrinkage
[a] 95% CI values were obtained from the sampling importance resampling (SIR) procedure
[b] IIV expressed as CV%

concentrations and HFS grades were simulated for 10,000 patients per dose-level, with a standardised body surface area of 1.75 m^2.

Model Selection and Evaluation

Discrimination between PK models was guided by physiological and scientific plausibility, general goodness-of-fit (GOF) plots, visual predictive checks (VPCs), precision of parameter estimates and change in objective function value (dOFV). A drop of ≥ 3.84, corresponding to a $P < 0.05$ (χ^2-distribution with 1 degree of freedom (df)), was considered a significant improvement of the fit for hierarchical nested models. The HFS models were evaluated by visual predictive checks (VPCs) by simulating 500 datasets and generating the 95% prediction intervals from these simulations. The observed proportion of patients with a certain HFS grade was compared with the simulated HFS grade over time. Additionally, predictive checks were performed by comparing the simulated and observed transitions between different HFS grades. Parameter precision was assessed by the sampling importance resampling (SIR) procedure (21).

Software

Nonlinear mixed-effects modelling was performed using NONMEM® (version 7.3, ICON Development Solutions, Ellicott City, MD, USA) and Perl-speaks-NONMEM (PsN, version 4.4.8) with First-Order Conditional Estimation with interaction (FOCE-I) as estimation method for the PK model. For the HFS model, the Laplacian method was used. Pirana (version 2.9.7) was used for model interpretation and comparison (22–24). R (version 3.4.3) was used for data management and graphical diagnostics (25).

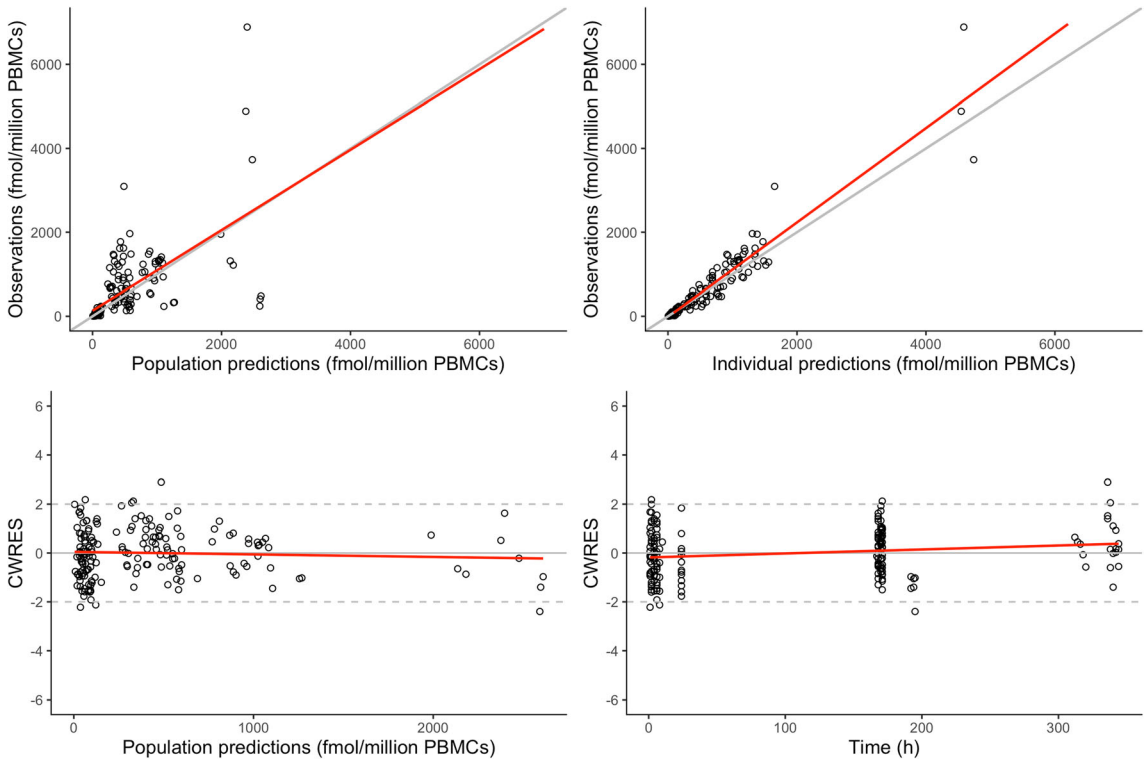

Fig. 2. Goodness-of-fit plots of the final PK model for intracellular FUTP concentrations. Including individual and population predictions *vs.* observed values and conditional weighted residuals (CWRES) *vs.* time after dose and PRED

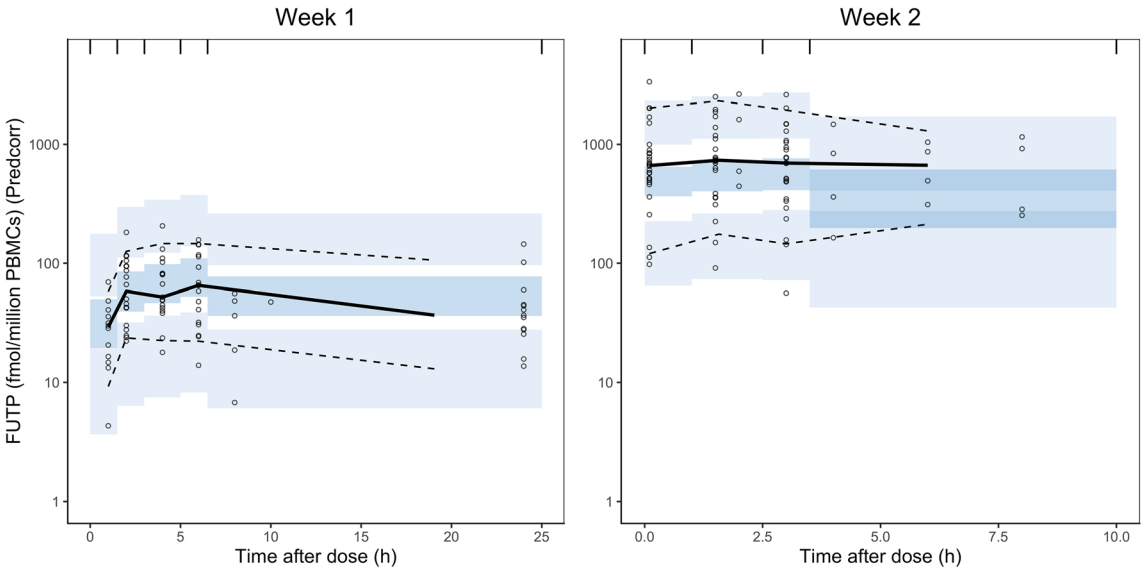

Fig. 3. Prediction-corrected visual predictive check of the final pharmacokinetic model for FUTP stratified by week, including the observed data from all three studies. Solid lines and darker blue areas represent the median observed values and simulated 95% CIs. Dashed lines and light blue areas represent the 5% and 95% percentiles of the observed values and the 95% CIs of the simulated percentiles ($n = 500$). CIs, confidence intervals

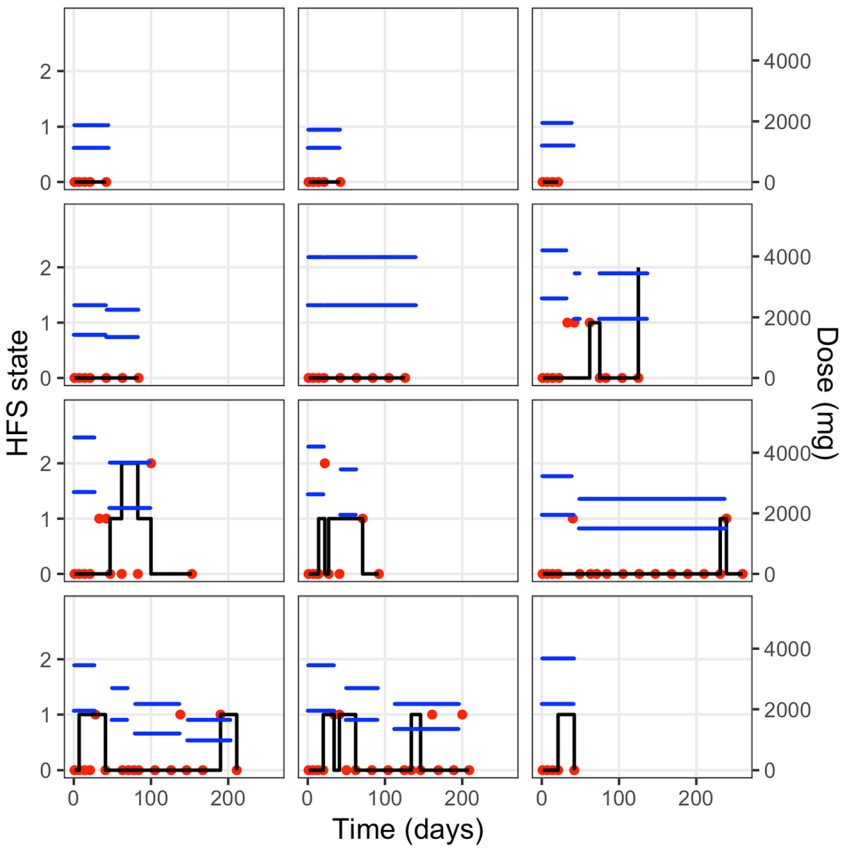

Fig. 4. Hand-and-foot syndrome (HFS) grade *versus* time profiles for 12 representative individual patients. State 0 is HFS grade 0/1, state 1 is grade 2 and state 2 is grade 3. Red dots are the observed HFS grades, solid black lines are the simulations from the continuous-time Markov model and blue horizontal lines represent the administered capecitabine daily doses

Table II. Estimates for the Final Markov Model for HFS

	Units	Estimate (95% CI[a])
Parameter		
Transition rate from grade 0/1 to 2 (k_{01})	week^{-1}	2.38×10^{-6} (4.56×10^{-7}–9.14×10^{-6})
Transition rate from grade 2 to 0/1 (k_{10})	week^{-1}	4.08×10^{-5} (2.10×10^{-5}–8.03×10^{-5})
Transition rate from grade 2 to 3 (k_{12})	week^{-1}	7.14×10^{-6} (1.20×10^{-6}–2.81×10^{-5})
Transition rate from grade 3 to 2 (k_{21})	week^{-1}	1.11×10^{-4} (2.71×10^{-5}–3.70×10^{-4})
Direct effect FUTP (E_{FUTP})[b]	fmol/million PBMCs	0.0023 (1.79×10^{-4}–1.33×10^{-2})

[a] 95% CI values were obtained from SIR
[b] Proportional effect of predicted FUTP concentrations

RESULTS

Intracellular Pharmacokinetic Model

A total of 175 PBMC samples were obtained from 45 patients and included in the analysis. Graphical inspection of the intracellular FUTP concentration-time data showed higher concentrations at day 7 compared to the first week after start of treatment. The model that best described these data was found to be a one-compartment model with first-order elimination ($k_{e,FUTP}$) where the rate of influx into PBMCs was directly proportional to the 5-FU plasma concentration; the final model structure is depicted in Fig. 1. (Eq. 3):

$$\frac{dC_{IC}}{dt} = k_{5\text{–}FU/FUTP} \cdot C_{5\text{–}FU} - k_{e,FUTP} \cdot C_{IC} \quad (3)$$

where C_{IC} represents the concentration in the intracellular FUTP compartment and $C_{5\text{-}FU}$ represents the 5-FU plasma concentration. The 5-FU plasma concentration was related to the intracellular FUTP concentration using a proportional model ($k_{5\text{-}FU/FUTP}$). Final parameter estimates are presented in Table I. $k_{5\text{-}FU/FUTP}$ was 0.029 h^{-1} × fmol/million PBMCs/nM (95% confidence interval (CI) 0.028–0.149 h^{-1} × fmol/million PBMCs/nM) and $k_{e,FUTP}$ was 0.028 h^{-1} (95% CI 0.022–0.039 h^{-1}) which corresponds to a FUTP elimination half-life of 24 h. IIV was identified for $k_{5\text{-}FU/FUTP}$ (66.0% (95% CI 53.1%–84.8%)) and could not be estimated for $k_{e,FUTP}$. The final model adequately predicted the FUTP concentrations over time, as shown by the GOF plots (Fig. 2) and VPC (Fig. 3). Figure 3 also shows that the increased concentrations in the second week of treatment are well predicted by the model.

HFS

HFS data were available only for the 24 patients that were included in study 1. In order to estimate the probability of observing each HFS grade at every observation, the HFS grades were modelled as differential equations including transition rates to- and from neighbouring grades (k_{01}, k_{10}, k_{12}, k_{21}) (20).

When including an univariate direct effect of capecitabine, 5-FU and FUTP concentrations on the increasing transition rates, an improvement of the HFS model fit was observed compared to the model without an effect of capecitabine PK (dOFV = − 8.30 ($P = 0.0039$, df = 1) for capecitabine concentrations, dOFV = −8.44 ($P = 0.036$, df = 1) for 5-FU concentrations and dOFV = − 13.4 ($P = 0.0003$, df = 1) for FUTP concentrations). The data was best described by a model including a direct effect of predicted FUTP concentrations. Individual model fits from individuals representing both no changes in HFS observations, and the different HFS grades, are depicted in Fig. 4. An indirect effect using the AUC or by using an effect compartment did not significantly improve the models using 5-FU or FUTP as predictor. Adequate parameter precision could be obtained as depicted in Table II, with final parameter estimates within the obtained 95% confidence intervals. The VPC for the final Markov model for HFS (Fig. 5) showed that the model predicted percentage of patients experiencing HFS grades over time captures the observed data. Figure 6 shows

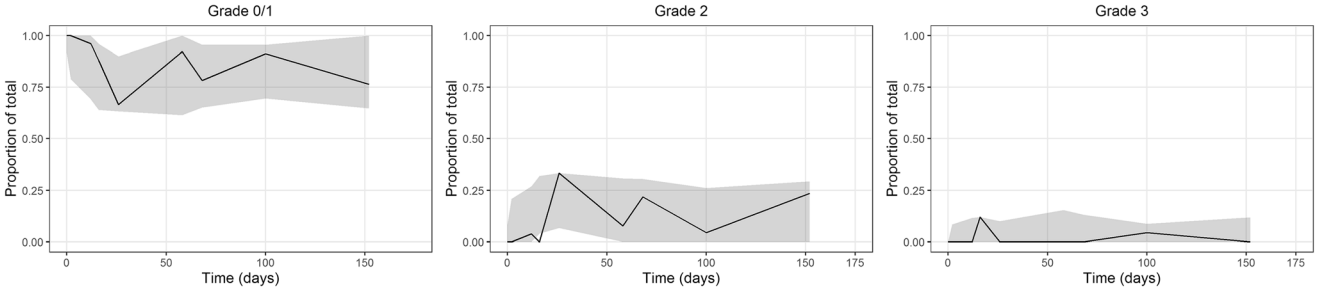

Fig. 5. Visual predictive check of the Markov model for capecitabine-induced hand-and-foot syndrome (HFS) grades stratified by grade. The grey areas represent the 95% prediction intervals for the proportion of patients developing HFS, and the solid lines represent the observed proportion of patients developing HFS ($n = 500$)

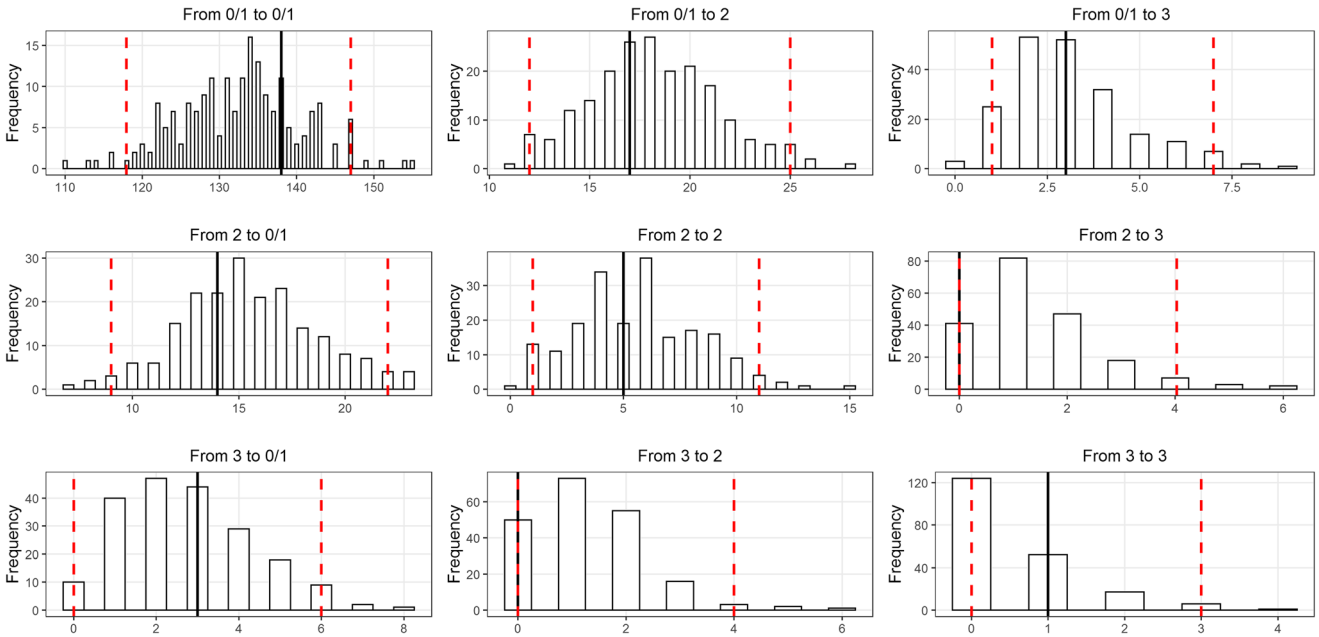

Fig. 6. Predictive check of the grade transitions for the Markov model for capecitabine-induced hand-and-foot syndrome including the intracellular FUTP effect. The histograms show the distribution frequency of the transitions simulated by the model ($n = 500$); the dashed lines represent the 5th and 95th percentiles of the simulations; and the solid line represents the observed number of transitions

the distribution frequency of the simulated and observed transitions for the final model. The 95% prediction intervals calculated from the simulated transitions adequately captured the observed number of transitions from one grade to another. Figure 7 shows the simulated proportions of clinically most relevant HFS grades (grades 2 and 3) on day 21 after the start of continuous treatment with capecitabine for five different dosing regimens, without taking into account clinically indicated treatment interruptions or dose adjustments. The percentage of patients experiencing grades 2 or grade 3 increased with higher dose regimens. The percentage of patients increased from 8.93 to 13.3% for grade 2 and from 1.22 to 2.66% for grade 3 when comparing the 375/625 mg/m^2 and 950/1600 mg/m^2 dosing regimens. Nevertheless, grade 3 HFS was simulated for a small number of patients. This is roughly in line with the HFS observations from study 1, where grade 3 HFS was only observed at the highest dose-level ($n = 3$, dose-level 950/1600 mg/m^2). The simulations additionally showed the delayed effect of FUTP on the development of HFS (supplemental Fig. S1). The percentage of patients experiencing grade 2 or 3 HFS increased with time and seems to be on a plateau after day 21, in the absence of treatment interruptions or dose adjustments.

DISCUSSION

A PK model that represents the FUTP concentrations in PBMCs of patients treated with capecitabine was successfully developed. The production of intracellular FUTP concentrations was described by a model where the plasma 5-FU concentrations drive the intracellular FUTP concentrations. FUTP elimination was characterised by a half-life of 24 h.

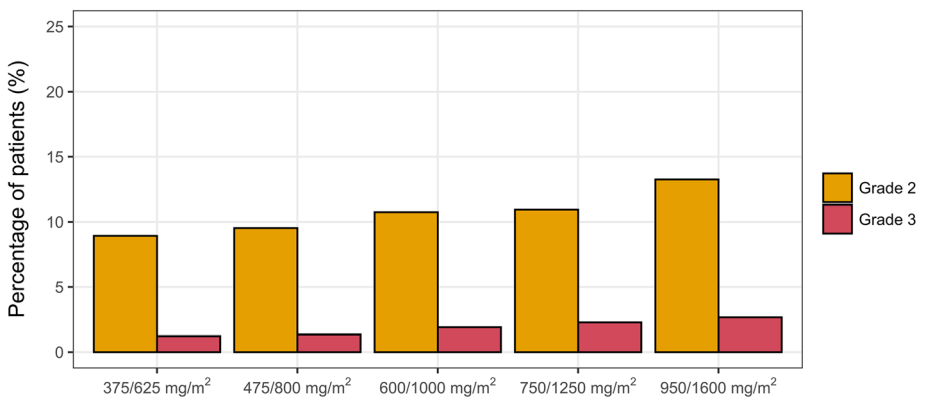

Fig. 7. Simulated percentage of patients experiencing HFS grades 2 and 3 on day 21 after the start of treatment with capecitabine for the dose-levels that were evaluated in study 1 ($n = 10{,}000$ per dose-level)

In addition, a CTMM characterised the onset and grade of HFS. The collection of toxicity data in our study had a non-uniform frequency, with weekly observations during the first 3 weeks of treatment followed by 3-weekly observations until the patient stopped treatment with capecitabine. The CTMM was thus used to describe the dynamics of HFS during treatment with capecitabine. The model-derived individual intracellular FUTP concentration was identified as the best predictor of the development and grade of HFS in this patient population. Models describing HFS by including capecitabine and 5-FU plasma concentrations as predictor did not result in an improvement of the model fit compared to a model with intracellular FUTP concentrations as predictor. Simulations showed an increased percentage of patients experiencing clinically relevant HFS with higher dosing regimens (grade 2 in 13.3% of patients dosed 950/1600 mg/m^2 compared to 8.93% of patients dosed 375/625 mg/m^2 and grade 3 in 2.66% of patients *versus* 1.22% of patients). Additionally, the cumulative effect of FUTP concentrations on the development of HFS was shown in the simulations. It should however be noted that a dose reduction or interruption would be applied when a patient experiences HFS in clinical practice, which was not included in our simulations. Previously, a model that describes the risk of developing HFS driven by plasma exposure to capecitabine has been developed (9). However, this model was only informed by dosing history without actual PK data and did not investigate the effects of intracellular metabolites. HFS is most often observed after patients have been on capecitabine therapy for several days or weeks emphasizing the delayed nature of HFS. It has therefore been hypothesised that HFS is a result of accumulation of capecitabine metabolites. Our analysis supports this latter hypothesis as intracellular FUTP concentrations related strongly to HFS. Due to the long half-life of intracellular FUTP, this metabolite shows accumulation during treatment, which also is in agreement with the observed cumulative nature of HFS.

The current analysis does harbour some limitations. Firstly, the intracellular concentrations that we used were measured in PBMCs and not in actual target tissue cells. Direct measurement of capecitabine and metabolite concentrations in skin samples might gain additional information for the here proposed model. However, this is impractical, highly invasive and therefore very difficult to perform in patients experiencing HFS. In addition, intracellular concentrations of the intermediate metabolites FUMP and FUDP were not detectable and therefore not included in the model. However, given the extremely low concentrations of these metabolites compared to FUTP, the role of these metabolites in HFS is questionable (2). Secondly, as a result of limited data, we decided to combine grade 0 and grade 1 into one category. This was considered reasonable since dose reductions and delays are only clinically indicated at grade 2 or higher. Lastly, we could not identify additional covariates in either the PK or the Markov model because they were unavailable for the PK dataset. Hypothetically, covariates such as genetic predispositions, renal function and baseline characteristics could influence the development of HFS and therefore improve the here presented models.

CONCLUSION

The here proposed integrated PK-PD model shows that, during capecitabine treatment, intracellular FUTP concentrations accumulate over time and are associated with the development and severity of HFS, which strengthens the hypothesis that HFS is a result of intracellular FUTP accumulation. In addition, this is the first analysis that demonstrates a clinically relevant relationship between intracellular FUTP concentrations following clinically relevant capecitabine dose regimens and HFS. The developed model can be used for simulation purposes such as the evaluation of the effect of alternative capecitabine dosing strategies on the development of HFS, the time-course of HFS disappearance after a dose reduction and overall optimisation of capecitabine treatment.

ACKNOWLEDGEMENTS

The authors thank the Research HPC facility of the Netherlands Cancer Institute for support in the use of computational resources.

COMPLIANCE WITH ETHICAL STANDARDS

Conflict of Interest The authors declare that they have no conflict of interest.

REFERENCES

1. Reigner B, Blesch K, Weidekamm E. Clinical pharmacokinetics of capecitabine. Clin Pharmacokinet. 2001;40(2):85–104.
2. Derissen EJB, Jacobs BAW, Huitema ADR, Rosing H, Schellens JHM, Beijnen JH. Exploring the intracellular pharmacokinetics of the 5-fluorouracil nucleotides during capecitabine treatment. Br J Clin Pharmacol. 2016;81(5):949–57.
3. Longley DB, Harkin DP, Johnston PG. 5-Flourouracil: mechanisms of action and clinical strategies. Nat Rev Cancer. 2003;3:330–8.
4. Milano G, Mari M, Lassalle S, Formento J, Francoual M, Lacour J, *et al*. Candidate mechanisms for capecitabine-related hand-foot syndrome. Br J Clin Pharmacol. 2008;66(1):88–95.
5. Wilkes GM, Doyle D. Palmar-plantar erythrodysesthesia. Clin J Oncol Nurs. 2005;9(1):103–6.
6. Lin E, Morris JS, Ayers GD. Effect of celecoxib on capecitabine-induced hand-foot syndrome and antitumor activity. Oncology (Williston Park). 2002;16(12 Suppl No14):31–7.
7. Kara IO, Sahin B, Erkisi M. Palmar-plantar erythrodysesthesia due to docetaxel-capecitabine therapy is treated with vitamin E without dose reduction. Breast. 2006;15(3):414–24.
8. Zhang RX, Wu XJ, Wan DS, Lu ZH, Kong LH, Pan ZZ, *et al*. Celecoxib can prevent capecitabine-related hand-foot syndrome in stage II and III colorectal cancer patients: result of a single-center, prospective randomized phase III trial. Ann Oncol. 2012;23(5):1348–53.
9. Hénin E, You B, VanCutsem E, Hoff P, Cassidy J, Twelves C, *et al*. A dynamic model of hand-and-foot syndrome in patients receiving capecitabine. Clin Pharmacol Ther. 2009;85(4):418–25.
10. Gieschke R, Burger H, Reigner B, Blesch KS, Steimer J. Population pharmacokinetics and concentration – effect relationships of capecitabine metabolites in colorectal cancer patients. Br J Clin Pharmacol. 2002;55:252–63.
11. Schmulenson E, Krolop L, Simons S, Ringsdorf S, Yon-Dschun K, Jaehde U. Evaluation of patient-reported severity of hand-foot syndrome under capecitabine using a Markov modeling approach. Cancer Chemother Pharmacol. 2020;86:435–44.

12. Jacobs BAW, Deenen MJ, Joerger M, Rosing H, de Vries N, Meulendijks D, *et al*. Pharmacokinetics of capecitabine and four metabolites in a heterogeneous population of cancer patients: a comprehensive analysis. CPT Pharmacometrics Syst Pharmacol. 2019;8:940–50.
13. Deenen MJ, Meulendijks D, Boot H, Legdeur M-CJC, Beijnen JH, Schellens JHM, *et al*. Phase 1a/1b and pharmacogenetic study of docetaxel, oxaliplatin and capecitabine in patients with advanced cancer of the stomach or the gastroesophageal junction. Cancer Chemother Pharmacol. 2015;76(6):1285–95.
14. Jacobs BAW, Meulenaar J, Rosing H, Pluim D, Tibben MM, de Vries N, *et al*. A phase 0 clinical trial of novel candidate extended-release formulations of capecitabine. Cancer Chemother Pharmacol. 2016;77(6):1201–7.
15. Roosendaal J, Jacobs BAW, Pluim D, Rosing H, de Vries N, van Werkhoven E, *et al*. Phase I pharmacological study of continuous chronomodulated capecitabine treatment. Pharm Res. 2020;37(5):89.
16. Deenen MJ, Rosing H, Hillebrand MJ, Schellens JHM, Beijnen JH. Quantitative determination of capecitabine and its six metabolites in human plasma using liquid chromatography coupled to electrospray tandem mass spectrometry. J Chromatogr B Anal Technol Biomed Life Sci. 2013;913–914:30–40.
17. Derissen EJB, Hillebrand MJX, Rosing H, Schellens JHM, Beijnen JH. Development of an LC–MS/MS assay for the quantitative determination of the intracellular 5-fluorouracil nucleotides responsible for the anticancer effect of 5-fluorouracil. J Pharm Biomed Anal. 2015;110:58–66.
18. Zhang L, Beal SL, Sheiner LB. Simultaneous vs. sequential analysis for population PK/PD data I: best-case performance. J Pharmacokinet Pharmacodyn. 2003;30(6):387–404.
19. Upton RN, Mould DR. Basic concepts in population modeling, simulation, and model-based drug development: part 3-introduction to pharmacodynamic modeling methods. CPT Pharmacometrics Syst Pharmacol. 2014;3(1):e88.
20. Schindler E, Karlsson MO. A minimal continuous-time Markov pharmacometric model. AAPS J. 2017;19(5):1424–35.
21. Dosne A-G, Bergstrand M, Karlsson MO. An automated sampling importance resampling procedure for estimating parameter uncertainty. J Pharmacokinet Pharmacodyn. 2017;44(6):509–20.
22. Lindbom L, Ribbing J, Jonsson EN. Perl-speaks-NONMEM (PsN)—a Perl module for NONMEM related programming. Comput Methods Prog Biomed. 2004;75(2):85–94.
23. Boeckmann AJ, Beal SL, Sheiner LB. NONMEM user's guide, part V. Intro Guide NONMEM Proj Gr. 1998;48.
24. Keizer RJ, van Benten M, Beijnen JH, Schellens JHM, Huitema ADR. Pirana and PCluster: a modeling environment and cluster infrastructure for NONMEM. Comput Methods Prog Biomed. 2011;101:72–9.
25. RC Team. R: a language and environment for statistical computing. Vienna: R Foundation for Statistical Computing; 2009.